Article

# Sonication-Induced, Solvent-Selective Gelation of a 1,8-Napthalimide-Conjugated Amide: Structural Insights and Pollutant Removal Applications

Apurba Pramanik, Basil Raju Karimadom, Haya Kornweitz, and Mindy Levine*

Read Online

ACCESS | 📊 Metrics & More | 📑 Article Recommendations | 🆘 Supporting Information

**ABSTRACT:** Reported herein is the synthesis, characterization, and dye removal applications of a highly solvent-selective organogel-forming amide, compound **1**, which contains a 1,8-naphthalmide moiety, flexible *n*-hexyl chain, and benzene ring. This compound displayed remarkable solvent selectivity, with gel formation occurring only in the presence of alkylated aromatic solvents. Detailed structural characterization of the gels, combined with notable theoretical insights, is invoked to explain the highly selective gelation properties of compound **1**, as is a comparison to non-gel forming structural isomer **2**, which contains the same structural elements in a different arrangement. Finally, the ability of the gel derived from compound **1** to act as a reusable material for the efficient removal of cationic organic dyes from contaminated aqueous environments is also reported, with up to 11 repeated uses of the gel still maintaining the ability to effectively remove Rhodamine B.
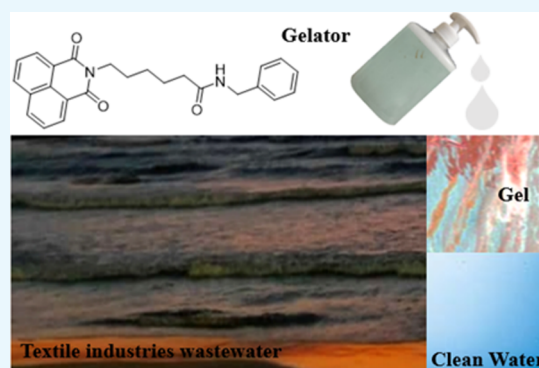
## INTRODUCTION

The ability to form supramolecular gels from the interaction of small organic molecules with organic[1] and aqueous solvents[2] has been studied extensively within the chemistry and material science communities,[3] and has been used in a variety of high-impact applications.[4−6] The optimization of such applications, including applications in thermal energy storage,[7] fluorescence detection,[8] and supramolecular catalysis,[9] are predicated on one's ability to understand how molecule−solvent interactions lead to gel formation, and how the structural features of both system components determine the propensity for gelation, the conditions under which gels form, and the stability and material properties of the resulting gels.[10] Nonetheless, much of the existing literature in the area of supramolecular gels relies on empirical observations (i.e., noticing that a particular compound interacts with a given solvent to form a gel), and lacks an understanding of the key structure−property relationships. Such an understanding, in turn, would directly enable accurate predictions of which compound−solvent combinations form gels, and ideally, what the properties of such gels would be.

One class of molecules with a known propensity for gelation are amides and amide-containing small molecules, oligomers, and polymers,[25] including peptides and proteins.[11] The fact that amides form organogels with a broad variety of solvents has sometimes been attributed to the highly polar nature of the amide bond that facilitates strong intermolecular interactions with polar organic solvents.[12] Moreover, the same polar amide bonds facilitate amide−amide interactions and concomitant supramolecular organization, which lead to trapping of a variety of solvents, particularly non-polar and aromatic solvents, within the ordered structure.[13] In many cases, however, the amide groups do not form intermolecular hydrogen bonds with the solvent, and gelation occurs via different interactions, such as aromatic[14] and heteroaromatic stacking interactions.[15] Such a supramolecular-induced structural order is particularly apparent in peptides and proteins that form α-helices, β-sheets, and β-strands,[16] but also occurs in non-peptide amides, particularly those with aromatic ring components that have the ability to participate in favorable π−π stacking interactions[17] in addition to the amide−amide interactions.[18]

A second class of compounds with a high propensity for gelation are naphthalimide-containing compounds.[19] These compounds, largely because of their large, flat aromatic structure, readily participate in π-π stacking interactions within or between the molecules, enabling the "trapping" of organic solvents within the ordered structure.[20] Moreover, because naphthalimide has a well-studied and highly tunable fluorescence emission profile,[21] structures containing naphthalimide can be characterized via fluorescence spectroscopy and/or

fluorescence-based microscopy,[22] and supramolecular structural changes (i.e., gelation and de-gelation) can be easily detected.[23]

Despite the significant interest in amide-containing small molecule gelators,[24] and the known ability of naphthalimide to participate in and/or induce gelation,[25] there are only isolated instances in which amide moieties and naphthalimides have been combined in the same gelator molecule.[26−28] Moreover, none of the reported instances of amide-containing naphthalimides investigate how structural modifications in the position of the amide bond affect gelation propensities. This is true despite the fact that achieving a detailed understanding around structure−property relationships in supramolecular gelators is expected to improve the fundamental understanding of non-covalent interactions involved in both gelation and de-gelation processes, as well as advance the pace of applications that rely on such gels.

Reported herein are the results of research conducted precisely to address this knowledge gap, by reporting the supramolecular gelation properties of naphthalimide-containing small molecule amide **1** (Figure 1). This structure forms highly
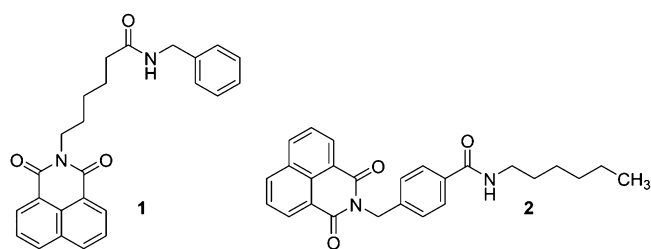
**Figure 2.** Absorbance (black line) and fluorescence emission (red line) spectra of compound **1** in chloroform ($[\mathbf{1}] = 1.18 \times 10^{-4}$ mM).

**Figure 1.** Structures of amides **1** and **2** investigated herein.

elastic organogels in the presence of alkyl-substituted aromatic solvents (and no organogels in the presence of other aromatic solvents and non-aromatic solvents), a result which can be explained based on theoretical calculations of its supramolecular ordering propensity. Full characterization of the gels formed from compound **1** are presented herein as well, as is its ability to bind and remove organic dyes from solution in a highly efficient, controlled, and reversible manner, with up to 11 cycles of gel washing and re-use presented. Computational investigations are invoked to explain the high solvent selectivity of compound **1**, and a comparison to non-gel forming compound **2** is used to provide additional scientific insights. Moreover, additional comparisons to compounds **15** and **16**, with shorter aliphatic linkers, provide specific insights about the effect of the linker length.

## RESULTS AND DISCUSSION

The UV−visible absorption and fluorescence emission spectra of compound **1** in chloroform showed the expected fine structure characteristic of naphthalimide-containing molecules (Figure 2),[29,30] with limited changes in these spectra over a wide range of concentrations indicative of limited aggregation in chloroform solutions (see Supporting Information for more details).

Interestingly, sonicating a solution of compound **1** ($[\mathbf{1}] =$ 0.025 M) in alkyl-substituted aromatic solvents (toluene, *o*-xylene, *m*-xylene, *p*-xylene, mesitylene, and ethyl benzene) led to the formation of an opaque organogel, as determined through the vial inversion test (Figure 3A). This gel was characterized in a number of ways, including through scanning electron microscopy (SEM) (Figure 3B), which shows the formation
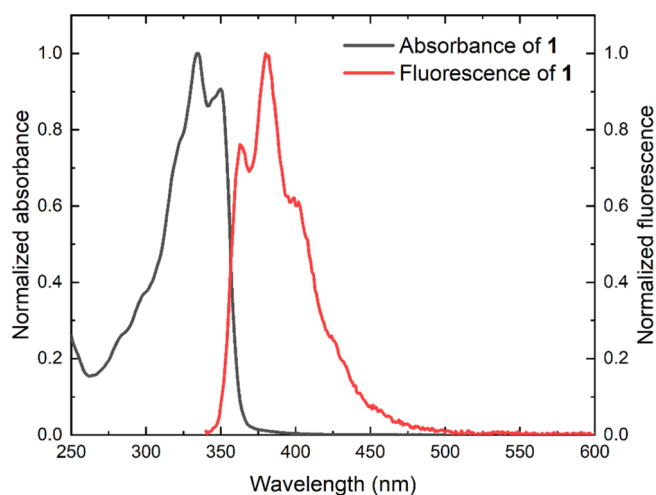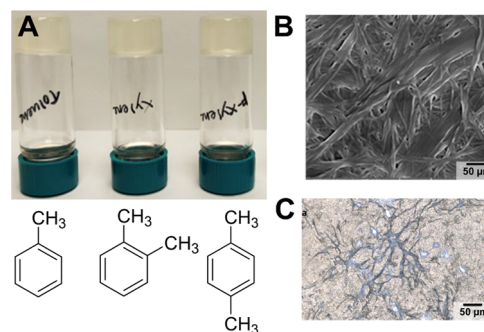
**Figure 3.** Confirmation of the formation of organogels derived from compound **1**. (A) Formation of a gel after mixing compound **1** with (L-to-R) toluene, *o*-xylene, or *p*-xylene, as shown through the inverted vial test; (B) SEM image of the gel formed from compound **1** and toluene; and (C) polarized optical microscopy images of a gel formed from compound **1** and *o*-xylene.

of an entangled fibrous network when compound **1** is sonicated with toluene; through polarized optical microscope images (Figure 3C); and after absorption of rhodamine B dye by the organogel (see Supporting Information for more details). Finally, the elastic nature of the gel derived from compound **1** was confirmed by rheology studies, which determined that the storage modulus ($G'$) was greater than the loss modulus ($G''$), indicating a highly elastic material.

Notably, this gelation was both solvent- and structure-specific. Other aromatic solvents, including benzene and a variety of halogen-substituted benzene derivatives, led to no gelation, nor did mixing with polar organic solvents (alkanols, acetonitrile, dichloromethane) and nonpolar aliphatic solvents (i.e., cyclo-hexane, *n*-hexanes, *n*-heptane). Interestingly, despite the high degree of structural similarity between compounds **1** and **2**, compound **2** did not induce gelation for any of the investigated solvents (see Supporting Information for a full list), resulting instead in either clear solutions, insoluble mixtures, or cloudy suspensions from which a solid powder precipitated over time (Figure 4).

Once a gel derived from compound **1** and alkylated aromatic solvents was successfully formed, potential applications of the gel were investigated, with a particular focus on the ability of the organogel to purify contaminated aqueous samples. This
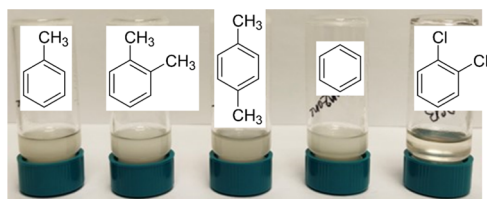
**Figure 4.** Lack of gelation seen when mixing compound **2** with aromatic solvents after sonication. (Left-to-Right): toluene, o-xylene, p-xylene, benzene, 1,2-dichlorobenzene.

application was facilitated by the fortuitous observation that in biphasic mixtures of aromatic solvents and water, compound **1** interacts only with the aromatic solvent to form a gel, and the aqueous layer remains unaffected (see Supporting Information for more details). This opens the possibility of using such organogels, with their high aqueous stability, for the removal of aqueous phase pollutants. To investigate this application, we prepared a variety of cationic aqueous dye solutions (as representative organic contaminants), and mixed the organogel formed from compound **1** and o-xylene with the solutions. Of note, the selection of cationic dyes exclusively was due to the known strength and versatility of the cation-$\pi$ interaction, and the expectation that the aromatic components of the organogel will interact favorably with the cationic components of the dyes investigated herein. The absorbance of the dye in solution over time was then recorded, with decreasing absorbance of the dye in solution indicating effective removal from solution and adsorption of the dye to the gel.

For all dyes investigated (compounds **10−14**, Figure 10), we determined that the gel formed from compound **1** and o-xylene effectively removed the dyes from water over a period of up to 72 h (Table 1). Of note, the efficiency of such removal depended

**Table 1. Removal of Dyes from Aqueous Solutions after Treatment with Organogel Formed from Compound 1 and o-Xylene, as Measured by the Normalized Integrated Absorbance of the Dye Remaining in Solution[a]**

| dye | removal time (h) | normalized integrated absorbance of the dye in solution[b] |
|---|---|---|
| methyl orange **10** | 60 | $0.39 \pm 9.4 \times 10^{-8}$ |
| methyl violet **11** | 72 | $0.26 \pm 2.4 \times 10^{-7}$ |
| **rhodamine B 12** | **48** | $0.01 \pm 1.2 \times 10^{-5}$ |
| rhodamine 6G **13** | 60 | $0.47 \pm 2.4 \times 10^{-8}$ |
| thioflavin T **14** | 72 | $0.40 \pm 5.7 \times 10^{-4}$ |

[a]The gel was formed from mixing 7.5 mg of compound **1** with 0.75 mL of o-xylene. Integration of the absorbance spectra was done from 250−500 nm, using wavenumbers on the X-axis and OriginPro software. [**10**] = [**11**] = [**12**] = [**13**] = [**14**] = 1 mg/mL. [b]The integrated absorbance was normalized so that the initial absorbance of the dye in solution was set to 1.0.

strongly on the identity of the dye, with rhodamine B showing complete removal from solution after 48 h (Figure 5A). In contrast, the least efficient dyes, rhodamine 6G and thioflavin T, showed removal from solution of up to 53 and 60%, respectively, even after a longer time period of mixing the gel with the solution (see Supporting Information for more details).

The practical applicability of such gels for pollutant removal efforts is dramatically enhanced in situations in which the gel can

be used for multiple pollutant removal cycles. To that end, a gel formed from compound **1** and o-xylene was first used to remove rhodamine B **12** from aqueous solution, according to the procedures detailed above. After effective adsorption of the dye to the gel, the gel was removed from the solution. In a separate step, the water-soluble dye was extracted into an aqueous solvent, and the compound **1**-derived organogel was disassembled in ethyl acetate. The recovered amide **1** was then used to re-form an organogel with o-xylene, and the resulting gel was used for another cycle of rhodamine B removal from contaminated aqueous solutions. This gel remained effective in removing rhodamine B from solution, although the percent recovery of amide **1** diminished with each repeat cycle (Figure 6). By the start of the fourth cycle, therefore, only 53% of the initial amount of compound **1** remained. These results show good initial data that gel reusability is feasible, and efforts to optimize this reusability cycle are currently underway in our research group. Moreover, preliminary data also demonstrated that the newly formed organogels could undergo self-healing, with two distinct gel segments (one with adsorbed dye and one without such dye) undergoing adhesion in the span of 15 min (see Supporting Information for more details).

Despite the high performance of compound **1** in forming organogels that act as effective, reusable pollutant removal materials, questions remain about the differential gelation propensities of compounds **1** and **2**, which occur despite their significant structural similarity. Such differences were investigated using both experimental and computational studies, with experimental investigations including solid-state Fourier transform infrared (FTIR) spectroscopy, powder X-ray diffraction (P-XRD), circular dichroism (CD) spectroscopy, and a variety of microscopic imaging techniques. These experiments highlighted the following key differences between compounds **1** and **2** that affect their supramolecular gelation properties:

1. Stronger hydrogen bonds in compound **2**. Evidence of such hydrogen bonds is seen in the differences in the amide I bands of the two compounds in their FTIR spectra, with the amide III band of compound **1** found at a higher wavenumber than the corresponding band in compound **2** (3300 cm$^{-1}$ vs 3310 cm$^{-1}$) (Figure 7A). Similarly, the position of the amide I band likewise differed between the two small molecule amides, with compound **1** showing a peak at 1660 cm$^{-1}$ and compound **2** showing one at 1630 cm$^{-1}$.

2. Sheet, microsphere, and crystalline formation for compound **2** aggregates compared to interlocked fibers for compound **1** aggregates. Most conclusively, SEM images of compound **2** mixed with aromatic solvents show crystalline morphologies (Figure 7B), sheet-like morphologies (Figure 7C), or microsphere morphologies (see Supporting Information). None of these morphologies seen through SEM have visibly interlocking fibers that enable the formation of a strong, elastic, organogel. In contrast, SEM images of compound **1** mixed with toluene (Figure 3B) showed clear images of interlocked fibers that support the macroscopically observed gel formation.

**Significance of Alkyl Chain Length.** In addition to amides **1** and **2**, discussed in detail above, we synthesized compounds **15** and **16**, amide analogs with shorter aliphatic linkers, instead of the six-carbon linkers found in amides **1** and **2** (Figure 8). Notably, neither **15** nor **16** formed organogels upon mixing with a range of organic solvents. We explain the lack of gelation of
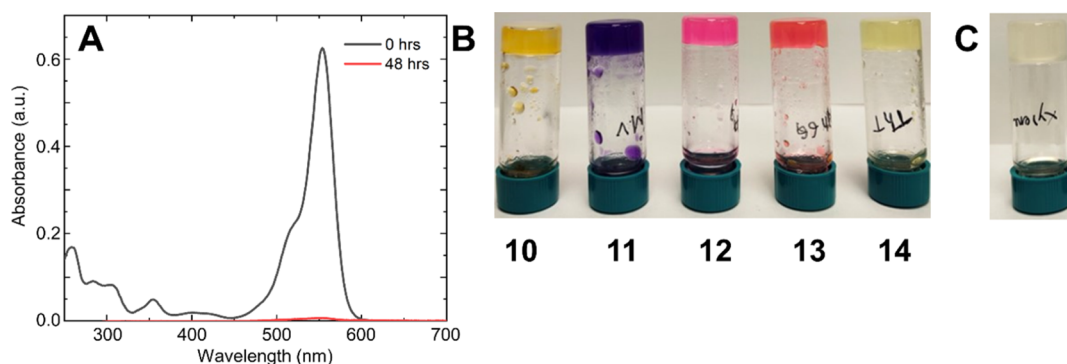
**Figure 5.** (A) Illustration of the removal of rhodamine B from contaminated aqueous solutions, as seen through changes in the UV−visible absorbance of the dye in a gel-treated solution at 0 h (black line) and 48 h (red line); (B) photograph of gels derived from compound **1** and *o*-xylene after absorbing dyes from contaminated aqueous solutions. (Left-to-Right: methyl orange **10**, methyl violet **11**, rhodamine B **12**, rhodamine 6G **13**, and thioflavin T **14**); and (C) Photograph of the gel formed from compound **1** and *o*-xylene before dye absorption occurs.
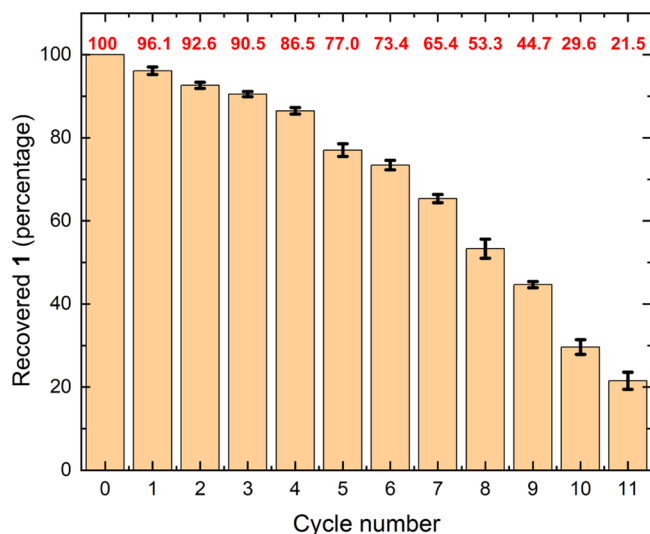


**Figure 6.** Summary of the percent recovery of compound **1** during its reuse for 11 cycles of pollutant removal applications.
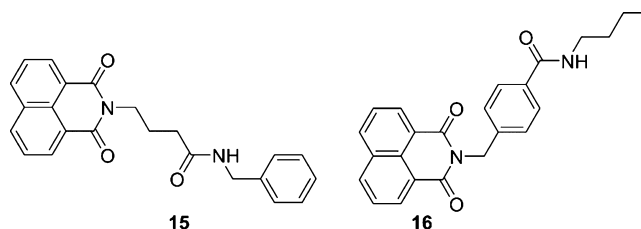


**Figure 8.** Structures of short-chain amide analogs **15** and **16**.

compound **15** as potentially due to steric repulsion between the bulky aromatic moieties that cannot be alleviated due to the short chain length. The lack of gelation behavior observed in compound **16** is explained much like the behavior of compound **2**, namely, that high rigidity in the structures precludes the intermolecular interactions that are necessary to achieve effective gelation.

Additionally, significant computational work uncovered quantitative differences between compounds **1** and **2**. Density functional theory (DFT) calculations of the dimers formed from compounds **1** and **2** indicated highly favorable dimer formation (i.e., negative binding energies) for compound **1** in vacuum, and in the presence of aromatic solvents benzene, toluene,
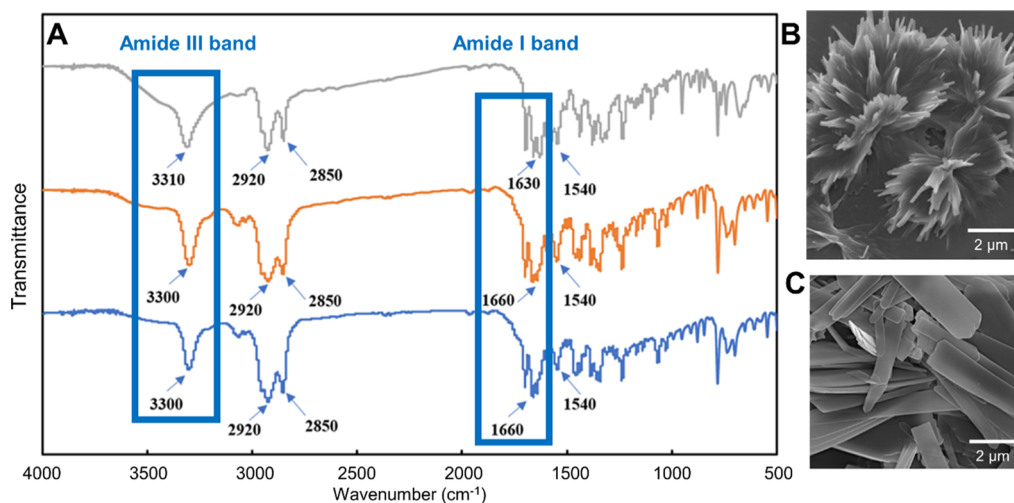


**Figure 7.** (A) Illustration of how differences in FTIR spectra indicate differences in the strength of hydrogen bonds. (Gray line: compound **2**; Orange line: organogel derived from compound **1**; blue line: compound **1**); (B) SEM image of compound **2** with 1,2-dichlorobenzene, forming a flower-like (i.e., non-gel) morphology; and (C) SEM image of compound **2** with toluene, forming a sheet-like (i.e., non-gel) morphology.

mesitylene, and chlorobenzene (Table 2). In contrast, compound **2** displayed positive binding energies of dimerization

**Table 2. DFT-Calculated Binding Energies of Dimers Derived from Compounds 1 and 2[a]**

| medium | compound 1 (kcal/mol) | compound 2 (kcal/mol) |
|---|---|---|
| vacuum | −44.31 | 14.32 |
| benzene | −34.17 | 19.33 |
| toluene | −34.21 | 19.30 |
| mesitylene | −34.62 | 19.04 |
| chlorobenzene | −31.63 | 20.65 |

[a]All calculations were performed according to the procedures detailed in the Experimental Section. Negative values of such binding energies indicate energetically favorable dimerization.

in all media investigated, indicating that it does not undergo dimerization. The reason for this differential propensity for dimerization can be seen through investigating the computed structures of the dimer of compound **1** (Figure 9A) and compound **2** (Figure 9B), which highlight that compound **1** has a geometry that facilitates intermolecular hydrogen bonding and insertion of the benzene ring of the second monomer between two parallel rings of the first monomer. In contrast, in compound **2**, the fact that the carbonyl group is directly attached to the aromatic ring precludes geometries favorable for intermolecular hydrogen bonding and for the highly favorable aromatic ring insertion. Finally, additional computational work indicated the highly energetically favorable formation of trimers and tetramers of compound **1** (binding energy trimer = −53.51 kcal/mol; binding energy tetramer = −119.82 kcal/mol), highlighting the energetic favorability of forming compound **1**-derived aggregates, including organogels.

Of note, despite the fact that there are negative (i.e., energetically favorable) binding energies for compound **1** with both benzene and chlorobenzene, mixing compound **1** with these solvents did not result in gelation. Reasons for this discrepancy between the computed properties and experimentally observed phenomena in this case are currently under investigation, although we hypothesize that it is likely due to the notable differences in electron density around the aromatic ring. Alkylated aromatic rings, with higher electron density, facilitate gelation with electron-deficient aromatic amides, whereas benzene and chlorobenzene, with lower electron density, do not undergo the same intermolecular interactions required for effective gelation to occur.

## CONCLUSIONS

Reported herein is the formation of elastic organogels from compound **1** and a variety of alkylated aromatic solvents, and the use of those gels for the effective removal of small molecule organic dyes from contaminated aqueous environments. Insights into the structural dependence of such gelation focus on the ability of compound **1** to form strongly energetically favorable hydrogen-bonded dimers and oligomers, in contrast to structurally related compound **2** which lacks such energetic favorability upon aggregation. Preliminary efforts are also presented toward the development of a reusable pollutant removal system, which has significant potential in the development of practical, real-world applications. Efforts toward realizing such applications are currently underway in our laboratory, as are efforts to extend the pollutant removal efforts to non-cationic (i.e., neutral and anionic) organic components, and the results of these and other investigations will be reported in due course.

## EXPERIMENTAL SECTION

**Materials and Methods.** All chemicals were purchased from commercial suppliers and used without further purification. All UV/visible absorption spectra were recorded on a Varian Cary 50 Bio UV−visible spectrophotometer. Fluorescence spectra were recorded on a Varian Cary Eclipse fluorescence spectrophotometer. ^{1}H NMR spectra were obtained using a Bruker AVANCE III spectrophotometer operating at 400 MHz and were referenced to signals from the deuterated solvents. The morphologies of the reported peptides were investigated using SEM (TESCAN MAIA3 Triglav). Polarized optical microscopic images were taken at 20-fold magnification (ZEISS, Axioscope 5 with polarizer and CCD camera). DLS experiments were performed using a NANO-PHOX SYMPA TC instrument. The rheological measurements were performed on a MCR 102 rheometer (Anton Paar, Modular Compact Rheometer) with a steel parallel plate geometry having 40 mm diameter at 25 °C. The rheometer was attached to a Peltier circulator thermocube in order to control the temperature. All CD experiments were conducted on a JASCO spectrophotometer. P-XRD data were taken using a Rigaku powder X-ray diffractometer.

**Synthesis of Compounds 1 and 2.** Compound **1** was accessed through the conversion of 1,8-naphthalic anhydride to naphthalimide **5**, followed by a DCC and HOBt-mediated amide coupling to access the target molecule **1** in 47% overall
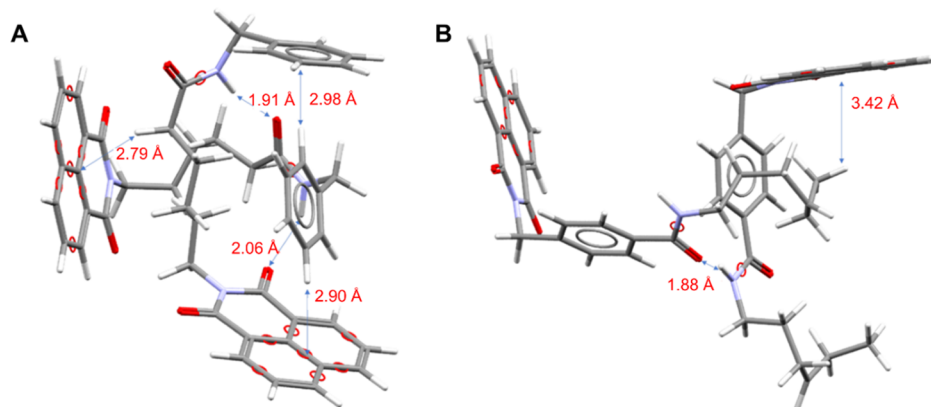


**Figure 9.** DFT-calculated geometries of dimers derived from (A) compound **1**; and (B) compound **2**.

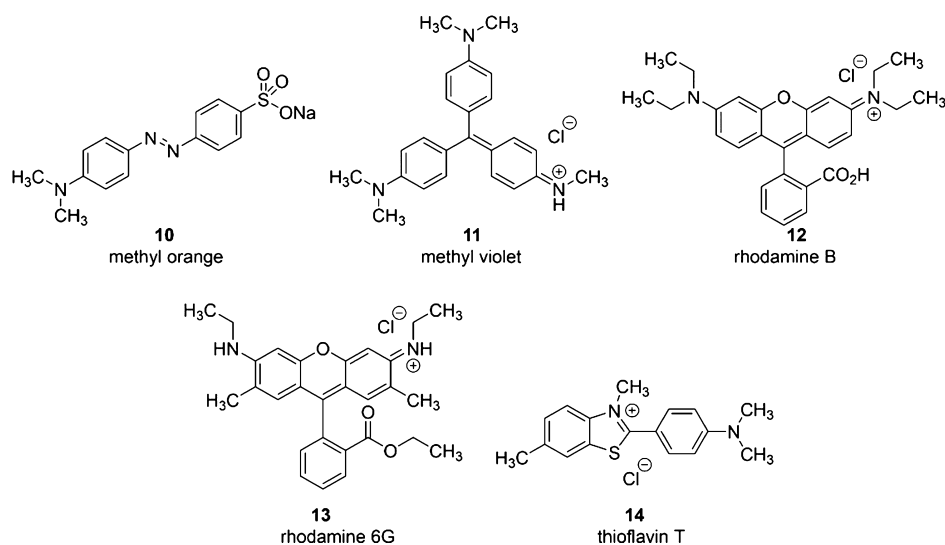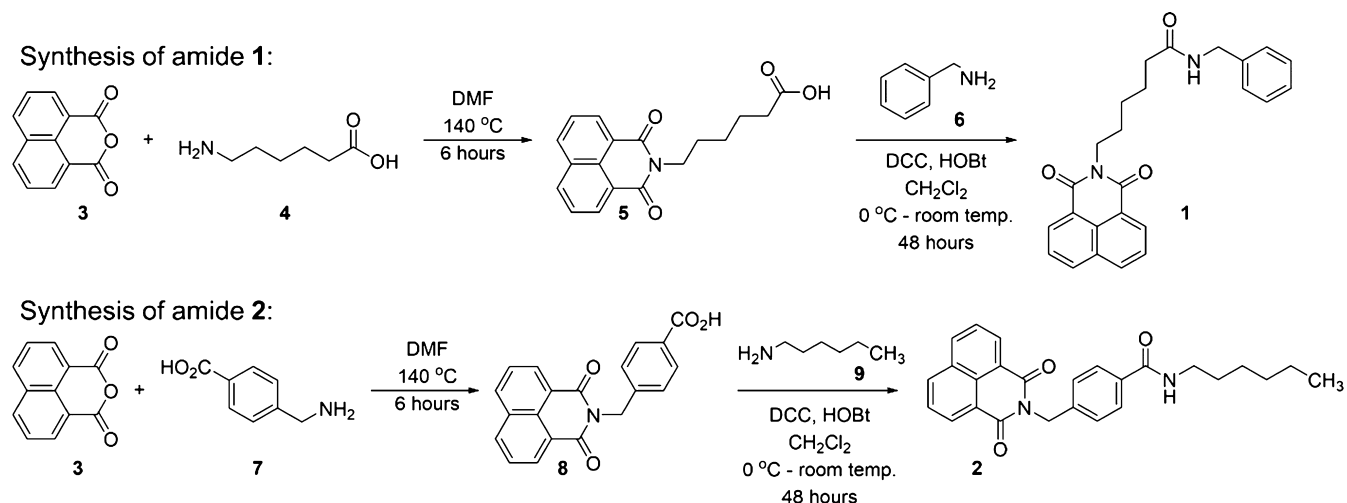**Scheme 1. Synthesis of Amides 1 and 2**





**Figure 10.** Structures of small molecules dyes used for dye uptake studies with organogels.

yield from commercially available starting materials (Scheme 1). Compound **2** was accessed via the transformation of 1,8-naphthalic anhydride to naphthalimide **8**, followed by DCC and HOBt mediated coupling to access compound **2** in 56% overall yield (Scheme 1). All intermediates and final products were characterized using $^1$H NMR spectroscopy, $^{13}$C NMR spectroscopy, and mass spectrometry (see Supporting Information for more details).

**Experimental Procedures for Aggregation Studies.** The concentrations of compounds **1** and **2** were varied between $4.51 \times 10^{-2}$ and $1.19 \times 10^{-1}$ mM, and the UV−visible and fluorescence spectroscopic properties of each solution were measured. Fluorescence emission spectra were collected following excitation at 330 nm.

**Experimental Procedures for Solid-State FTIR Studies.** Compounds **1** and **2**, as well as a gel derived from sonicating compound **1** in toluene, were studied using solid-state FTIR spectroscopy. KBr pellets of each substance were formed, and spectra were collected after the appropriate background and control scans.

**Experimental Procedures for Gelation Studies.** Detailed gelation studies were conducted by sonicating a solution of each compound in an organic solvent (for sonication-induced gelation) or by heating the solution of each compound in an organic solvent to 90−100 °C, followed by slowly cooling to room temperature (for heat-induced gelation). Gel formation was measured by inverting the vial and determining if the material remained at the top of the vial (indicating that a gel had formed) or if it fell to the bottom of the vial (indicating the existence of a solution or cloudy suspension).

**Experimental Procedures for Dye Uptake Studies.** Dye uptake studies were conducted by mixing a solution of compound **1** with $o$-xylene to create an organogel, followed by adding a solution of the dye (compounds **10–14**, Figure 10). Uptake of the dye was measured by monitoring changes in the UV−visible absorbance spectrum over time.

**Experimental Procedures for Gel Reusability Studies.** The potential for reusability of the organogels was measured by investigating the uptake of compound **12** by a gel formed from compound **1** and $o$-xylene, followed by removing the dye from the gel and re-using the gel for another round of dye uptake.

**Experimental Procedures for Imaging Studies.** Imaging studies were conducted using a scanning electron microscope

after thorough drying of the samples under vacuum, followed by gold coating prior to imaging.

**Experimental Procedures for Rheology Studies.** Rheology experiments were conducted using small amounts of the gel formed from compound **1** in toluene, *o*-xylene, and *m*-xylene, in which the storage modulus ($G'$) and loss modulus ($G''$) of the gel were measured as a function of angular frequency.

**Experimental Procedures for CD Studies.** CD studies were performed by measuring the spectra of compounds **1** and **2** in methanol ($[\mathbf{1}] = [\mathbf{2}] = 4.51 \times 10^{-2}$ mM).

**Experimental Procedures for P-XRD Studies.** The powder XRD patterns of samples of compound **1**, compound **2**, and a gel formed between compound **1** and *o*-xylene were measured after each sample was carefully dried under vacuum and ground with a mortar and pestle.

**Procedures for Quantum Chemical Calculations.** Quantum chemical structural optimizations were carried out using a Gaussian 16 program.[31] All structures were fully optimized with Khon−Sham DFT, using hybrid functional of B3LYP in combination with Poples's basis set 6-311G(d,p).[32,33] The effects of dispersion were integrated using Grimmies's D3 dispersion with the Becky-Johnson damping.[34] A Truhlar's SMD solvation model was used to consider the implicit solvation effects.[35] Once the structural optimizations converged, the vibrational frequency analysis was performed with the same level of theory to ensure that the final point is a real minima ($N_{\text{img}} = 0$).

## ASSOCIATED CONTENT

### Ⓢ Supporting Information

The Supporting Information is available free of charge at https://pubs.acs.org/doi/10.1021/acsomega.1c04453.

> Detailed synthetic and experimental procedures, summary tables of all aggregation and gelation experiments, summary figures including all spectral data of newly synthesized compounds, UV−visible and fluorescence spectra, microscopy images, PXRD results, DLS results, and rheology experimental results (PDF)

## AUTHOR INFORMATION

### Corresponding Author

**Mindy Levine** − *Department of Chemical Sciences, Ariel University, Ariel 40700, Israel;* ⓘ orcid.org/0000-0003-4847-7791; Phone: 972535698117; Email: mindyl@ariel.ac.il

### Authors

**Apurba Pramanik** − *Department of Chemical Sciences, Ariel University, Ariel 40700, Israel*

**Basil Raju Karimadom** − *Department of Chemical Sciences, Ariel University, Ariel 40700, Israel;* ⓘ orcid.org/0000-0002-1674-7796

**Haya Kornweitz** − *Department of Chemical Sciences, Ariel University, Ariel 40700, Israel;* ⓘ orcid.org/0000-0002-3562-0141

Complete contact information is available at:
https://pubs.acs.org/10.1021/acsomega.1c04453

### Author Contributions

The manuscript was written through the contributions of all authors, and all authors have given approval to the final version of the manuscript.

### Notes

The authors declare no competing financial interest.

## ■ REFERENCES

(1) Ajayaghosh, A.; Praveen, V. K.; Vijayakumar, C. Organogels as Scaffolds for Excitation Energy Transfer and Light Harvesting. *Chem. Soc. Rev.* **2008**, *37*, 109−122.

(2) Lim, J. Y. C.; Goh, S. S.; Loh, X. J. Bottom-Up Engineering of Responsive Hydrogel Materials for Molecular Detection and Biosensing. *ACS Mater. Lett.* **2020**, *2*, 918−950.

(3) Fujita, N.; Mukhopadhyay, P.; Shinkai, S. Recent Development of Organogels Towards Smart and Soft Materials. *Annu. Rev. Nano Res.* **2006**, *1*, 385−428.

(4) Fameau, A.-L.; Rogers, M. A. The curious case of 12-hydroxystearic acid - the Dr. Jekyll & Mr. Hyde of molecular gelators. *Curr. Opinion Colloid Interface Sci.* **2020**, *45*, 68−82.

(5) Scharfe, M.; Flöter, E. Oleogelation: From Scientific Feasibility to Applicability in Food Products. *Eur. J. Lipid Sci. Technol.* **2020**, *122*, 2000213.

(6) Jayakumar, A.; Jose, V. K.; Lee, J.-M. Hydrogels for Medical and Environmental Applications. *Small Methods* **2020**, *4*, 1900735.

(7) Yazdani, M. R.; Ajdary, R.; Kankkunen, A.; Rojas, O. J.; Seppälä, A. Cellulose Nanofibrils Endow Phase-Change Polyethylene Glycol with Form Control and Solid-to-gel Transition for Thermal Energy Storage. *ACS Appl. Mater. Interfaces* **2021**, *13*, 6188−6200.

(8) Jo, S.; Ahn, H.; Park, S.-Y.; Lee, T. S. Synthesis of gelation-induced emissive, o-phenylazonaphthol-based organogel and its responsiveness to fluoride anion. *Tetrahedron* **2021**, *81*, 131895.

(9) Wang, G.; Wang, D.; Bietsch, J.; Chen, A.; Sharma, P. Synthesis of Dendritic Glycoclusters and Their Applications for Supramolecular Gelation and Catalysis. *J. Org. Chem.* **2020**, *85*, 16136−16156.

(10) Pradhan, B.; Vaisakh, V. M.; Nair, G. G.; Rao, D. S. S.; Prasad, S. K.; Sudhakar, A. A. Effect of Atomic-Scale Differences on the Self-Assembly of Thiophene-based Polycatenars in Liquid Crystalline and Organogel States. *Chem.—Eur. J.* **2016**, *22*, 17843−17856.

(11) Tan, T.; Shen, Z.; Wang, Y.; Guo, Z.; Hu, J.; Zhang, Y. Self-Assembly of Pentapeptides in Ethanol to Develop Organogels. *Soft Matter* **2020**, *16*, 10567−10573.

(12) Kumar, S.; Bera, S.; Nandi, S. K.; Haldar, D. The effect of amide bond orientation and symmetry on the self-assembly and gelation of discotic tripeptides. *Soft Matter* **2021**, *17*, 113−119.

(13) Ogi, S.; Stepanenko, V.; Sugiyasu, K.; Takeuchi, M.; Würthner, F. Mechanism of Self-Assembly Process and Seeded Supramolecular Polymerization of Perylene Bisimide Organogelator. *J. Am. Chem. Soc.* **2015**, *137*, 3300−3307.

(14) Li, Q.; Li, R.; Lan, H.; Lu, Y.; Li, Y.; Xiao, S.; Yi, T. Halogen Effect on Non-Conventional Organogel Assisted by Balanced $\pi$-$\pi$ Interaction. *ChemistrySelect* **2017**, *2*, 5421−5426.

(15) Diebold, M.; Christ, E.; Biniek, L.; Karmazin, L.; Heinrich, B.; Contal, C.; Ghosh, S.; Mesini, P. J.; Brinkmann, M. Original

polymorphism in a naphthalene bisimide π-conjugated organogelator: a complex interplay between hydrogen bonding and heterocycle π-stacking. *J. Mater. Chem. C* **2019**, 7, 13120−13129.

(16) Hermes, F.; Otte, K.; Brandt, J.; Gräwert, M.; Börner, H. G.; Schlaad, H. Polypeptide-Based Organogelators: Effects of Secondary Structure. *Macromolecules* **2011**, 44, 7489−7492.

(17) Lu, J.; Hu, J.; Liang, Y.; Cui, W. The Supramolecular Organogel Formed by Self-Assembly of Ursolic Acid Appended with Aromatic Rings. *Materials* **2019**, 12, 614.

(18) Fages, F.; Vögtle, F.; Žinic, M. Systematic Design of Amide- and Urea-Type Gelators with Tailored Properties. *Top. Curr. Chem.* **2005**, 256, 77−131.

(19) Liu, Y.; Liu, L.; Zhang, L.; Lv, X.; Che, G. A Monopyrrolote-trathiafulvalene Based Naphthalimide Tailored Organogelator with Stimuli Responsive Properties and Absorption for Rhodamine B. *Colloids Surf., A* **2020**, 584, 124053.

(20) Pham, Q. N.; Brosse, N.; Frochot, C.; Dumas, D.; Hocquet, A.; Jamart-Grégoire, B. Influence of the gelator structure and solvent on the organisation and chirality of self-assembling fibrillar networks. *New J. Chem.* **2008**, 32, 1131−1139.

(21) Udhayakumari, D. Various Sensing Mechanisms for the Design of Naphthalimide based Chemosensors Emerging in Recent Years. *Recent Innovations Chem. Eng.* **2020**, 13, 262−289.

(22) Cao, X.; Zhang, T.; Gao, A.; Li, K.; Cheng, Q.; Song, L.; Zhang, M. Aliphatic Amine Responsive Organogel System Based on a Simple Naphthalimide Derivative. *Org. Biomol. Chem.* **2014**, 12, 6399−6405.

(23) Pang, X.; Ge, J.; Yu, X.; Li, Y.; Shen, F.; Wang, Y.; Ren, J. An "off-on" fluorescent naphthalimide-based sensor for anions: its application in visual F− and AcO− discrimination in a self-assembled gel state. *New J. Chem.* **2019**, 43, 10554−10559.

(24) Rao, M. R.; Sun, S.-S. Supramolecular Assemblies of Amide-Derived Organogels Featuring Rigid π-Conjugated Phenylethynyl Frameworks. *Langmuir* **2013**, 29, 15146−15158.

(25) Dong, H.-Q.; Wei, T.-B.; Ma, X.-Q.; Yang, Q.-Y.; Zhang, Y.-F.; Sun, Y.-J.; Shi, B.-B.; Yao, H.; Zhang, Y.-M.; Lin, Q. 1,8-Naphthalimide-based fluorescent chemosensors: recent advances and perspectives. *J. Mater. Chem. C* **2020**, 8, 13501−13529.

(26) Kumar, M.; Sementa, D.; Narang, V.; Riedo, E.; Ulijn, R. V. Self-Assembly Propensity Dictates Lifetimes in Transient Naphthalimide-Dipeptide Nanofibers. *Chem.—Eur. J.* **2020**, 26, 8372−8376.

(27) Yang, H.-L.; Sun, X.-W.; Zhang, Y.-M.; Wang, Z.-H.; Zhu, W.; Fan, Y.-Q.; Wei, T.-B.; Yao, H.; Lin, Q. A bi-component supramolecular gel for selective fluorescence detection and removal of Hg2+ in water. *Soft Matter* **2019**, 15, 9547−9552.

(28) Feng, G.; Wang, Z.; Yu, X.; Lan, H.; Ren, J.; Geng, L.; Yi, T. An Ultrasound Triggered Gelation Approach to Selectively Solvatochromic Sensors. *Sens. Actuators, B* **2017**, 243, 1020−1026.

(29) Mukherjee, S.; Thilagar, P. Fine-tuning solid-state luminescence in NPIs (1,8-naphthalimides): impact of the molecular environment and cumulative interactions. *Phys. Chem. Chem. Phys.* **2014**, 16, 20866−20877.

(30) Mukherjee, S.; Thilagar, P. Insights into the AIEE of 1,8-Naphthalimides (NPIs): Inverse Effects of Intermolecular Interactions in Solution and Aggregates. *Chem.—Eur. J.* **2014**, 20, 8012−8023.

(31) Frisch, M. J.; Trucks, G. W.; Schlegel, H. B.; Scuseria, G. E.; Robb, M. a.; Cheeseman, J. R.; Scalmani, G.; Barone, V.; Petersson, G. a.; Nakatsuji, H.; Li, X.; Caricato, M.; Marenich, A. V.; Bloino, J.; Janesko, B. G.; Gomperts, R.; Mennucci, B.; Hratchian, H. P.; Ortiz, J. V.; Izmaylov, a. F.; Sonnenberg, J. L.; Williams-Young; Ding, F.; Lipparini, F.; Egidi, F.; Goings, J.; Peng, B.; Petrone, A.; Henderson, T.; Ranasinghe, D.; Zakrzewski, V. G.; Gao, J.; Rega, N.; Zheng, G.; Liang, W.; Hada, M.; Ehara, M.; Toyota, K.; Fukuda, R.; Hasegawa, J.; Ishida, M.; Nakajima, T.; Honda, Y.; Kitao, O.; Nakai, H.; Vreven, T.; Throssell, K.; Montgomery, J. a., Jr.; Peralta, J. E.; Ogliaro, F.; Bearpark, M. J.; Heyd, J. J.; Brothers, E. N.; Kudin, K. N.; Staroverov, V. N.; Keith, T. a.; Kobayashi, R.; Normand, J.; Raghavachari, K.; Rendell, a. P.; Burant, J. C.; Iyengar, S. S.; Tomasi, J.; Cossi, M.; Millam, J. M.; Klene, M.; Adamo, C.; Cammi, R.; Ochterski, J. W.; Martin, R. L.; Morokuma,

K.; Farkas, O.; Foresman, J. B.; Fox, D. J. *Gaussian 16*, Revision C.01; Gaussian, Inc.: Wallingford, G16_C01, 2016.

(32) Becke, A. D. Density-Functional Exchange-Energy Approximation with Correct Asymptotic Behavior. *Phys. Rev. A* **1988**, 38, 3098−3100 ; ISSN: 0556-2791.

(33) Lee, C.; Yang, W.; Parr, R. G. Development of the Colle-Salvetti correlation-energy formula into a functional of the electron density. *Phys. Rev. B: Condens. Matter Mater. Phys.* **1988**, 37, 785−789.

(34) Grimme, S.; Ehrlich, S.; Goerigk, L. Effect of the Damping Function in Dispersion Corrected Density Functional Theory. *J. Comput. Chem.* **2011**, 32, 1456−1465.

(35) Marenich, A. V.; Cramer, C. J.; Truhlar, D. G. Universal Solvation Model Based on Solute Electron Density and on a Continuum Model of the Solvent Defined by the Bulk Dielectric Constant and Atomic Surface Tensions. *J. Phys. Chem. B* **2009**, 113, 6378−6396.